J. Phys. B: At. Mol. Opt. Phys. **33** (2000) 3807–3823. Printed in the UK PII: S0953-4075(00)09268-3

Establishment of phase between coupled Bose–Einstein condensates

J A Dunningham and K Burnett

Clarendon Laboratory, Department of Physics, University of Oxford, Parks Road, Oxford OX1 3PU, UK

Received 4 November 1999

Abstract. We study how phase information is developed and transferred between Bose–Einstein condensates. First, we investigate how the phase of an output pulse of an idealized atom laser can be controlled. We then use quantum simulations to show how a relative phase between coupled systems is established by dissipation and atomic interactions. Our simulations show that each realization settles to the same relative phase between modes: for uncoupled systems the phase varies from realization to realization. We use this to demonstrate how condensates may 'naturally' possess a relative phase, and to explain the phase-locking mechanism in a recent experimental demonstration of a mode-locked atom laser.

1. Introduction

Several recent papers have discussed phase in mesoscopic Bose condensed systems [1–3]. They have shown that a relative phase between condensates is readily produced by measurement. In a recent paper we discussed a phase standard for Bose–Einstein condensates [4] based on the relative phase between condensates and the associated entanglement. This entanglement was produced by the phase measurement process itself and gave a definition of phase free from *ad hoc* assumptions about the initial state of the condensates involved. In this paper, we want to extend our analysis of phase to systems of coupled condensates. This is of special interest due to recent experimental advances in creating superpositions of condensates in two hyperfine levels [5] and chains of coupled trapped condensates [6]. In particular, we want to study how phase information is established and transferred between the condensates, both with and without the effects of dissipation.

In section 2, we begin by investigating the effect of a Josephson-like transfer on the phase of a condensate and see whether we can predict and control the phase of the transferred component. In section 3, we study how phase is transported along a set of coupled condensates if we make measurements which establish a phase at one site. Finally, in section 4, we extend this idea to demonstrate how dissipation and interactions can naturally give rise to phase in systems of coupled condensates. This has been inspired by a recent experimental demonstration of a mode-locked atom laser [6], in which the output from a lattice of coupled condensates is observed as a train of atomic pulses, providing a clear demonstration of phase-locking of the condensate modes.

0953-4075/00/193807+17$30.00

2. Phase of Josephson-transferred condensates

2.1. Introduction

Let us first discuss the form of the coupling between condensates. Josephson coupling [7] can be achieved through quantum mechanical tunnelling or by coupling with laser fields. Raman transfer, i.e. a stimulated transfer to another internal atomic state, can be brought about by applying two laser fields to a condensate [8]. This preserves the coherence and can be used for atomic beamsplitters [9] and output couplers for atom lasers [10].

Hall *et al* [11] used Raman pulses to create an interferometer by transferring half the population in a condensate to another trapped state. They then allowed the system to evolve before recombining the two components and studying the interference pattern in their region of overlap. Among other things, they demonstrated that the relative phase between the two components is fixed and repeatable. This means that one should be able to transfer a condensate into a number of different modes, all with the same phase relationship to the original.

The question arises as to whether we can go one step further and predict the value of the relative phase between the two components? It may seem obvious to some that the phase of the transferred component should be identical to that of the original. In fact, we shall show that it is not always so. In this section, we discuss simulations of the transfer process and investigate the reproducibility of the relative phase as well as its value. We also investigate how the phase depends on the system parameters and how to prepare condensates with a given phase relative to their mother. This is of particular interest in relation to the output pulses from atom lasers, since they rely on Josephson-like transfer as the output coupling mechanism [12].

2.2. Phase preparation

The first step in our scheme is to establish and measure a relative phase between the condensate and the phase standard. We follow a procedure similar to that outlined in previous work [4].

We consider three condensate modes, identified in turn with the annihilation operators a, b and c. Initially a and b are taken to be in number states and we allow outputs from these modes to be incident on the ports of a 50:50 beamsplitter (see figure 1). Detecting atoms at the two output ports entangles the modes as we cannot know from which mode an atom comes. This entanglement leads to the establishment of a relative phase between the modes. This is the temporal analogue of the measurement-induced entanglement scheme proposed by Javanainen and Yoo [1].

We use a quantum jump method [13], to keep track of the quantum state of the three-mode system at all times. This enables us to keep a full record of all the entanglements. If we transform to a frame rotating at the frequency of mode a, ω_a, the field operators at the two output ports of the beamsplitter, in the Heisenberg picture, are

$$C_1 = \sqrt{\kappa/2}\left(a + \mathrm{i}b\mathrm{e}^{-\mathrm{i}\Omega t}\right) \tag{1}$$

$$C_2 = \sqrt{\kappa/2}\left(\mathrm{i}a + b\mathrm{e}^{-\mathrm{i}\Omega t}\right) \tag{2}$$

where κ is the rate of detection of atoms, $\Omega = \omega_b - \omega_a$, and ω_b is the frequency of mode b.

The procedure for simulating this measurement process and keeping track of the quantum state of the system conditioned on all the previous detections, $|\psi_c\rangle$, is outlined in other work [4]. The state vector at the end of this process is

$$|\psi_c\rangle = \left(\sum_{i=N-l}^{N} d_i |2N - l - \mathrm{i}\rangle_a |i\rangle_b\right)|0\rangle_c \tag{3}$$

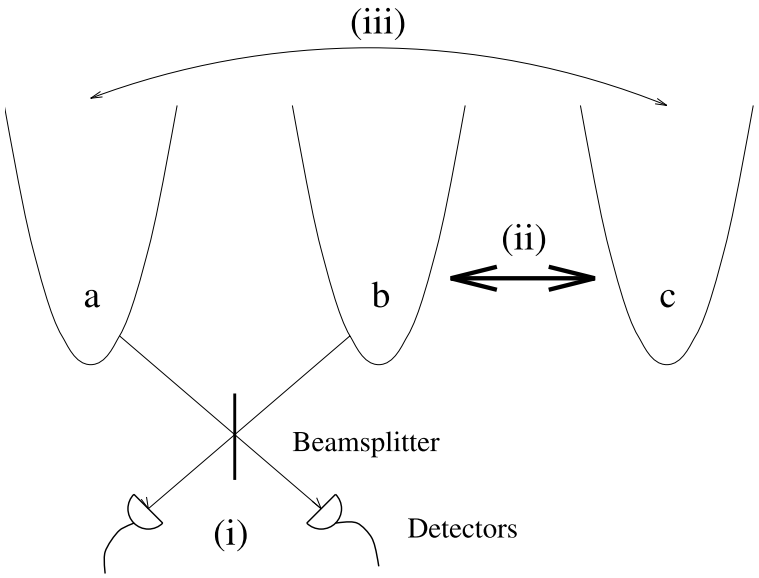

Figure 1. The three-mode set-up. (i) In the first stage, condensates a and b are the inputs to a beamsplitter and we record atomic detection times at the two output ports. (ii) In the second stage we Raman transfer part of mode b (now entangled with a) to mode c, which is initially empty. (iii) Finally, we measure the relative phase between a and c and also between a and b and compare with the results of the phase measurement in (i).

where N is the initial number of atoms in each of modes a and b, l is the number of atoms detected ($l < N$), and $\{d_i\}$ are the coefficients determined by the numerical simulation. Modes a and b are entangled by the measurement process, and mode c is unaffected.

Throughout the simulation, we calculate the relative phase between a and b. Mathematically, this can be written as

$$\phi_{ba}(t) = \arg\left\{\langle\psi_c(t)|a^\dagger b|\psi_c(t)\rangle\right\}. \tag{4}$$

Although this is not the most general definition of the phase [14], it is sufficient for our present purposes. The measurement scheme serves the dual role of both creating and measuring the relative phase. This phase (4) may be found by taking the difference in the number of atoms detected at each port, $D(t)$, per time interval, Δt. For zero phase difference, we would expect equal numbers of detections at each port, and for a leading (lagging) b by $\pi/2$ we would expect more detections at port 1 (2). This means that for non-degenerate modes we would expect to see a sinusoidal time dependence of the difference in numbers of atoms detected at the two ports. In analogy with the position of the spatial fringes in interference experiments, we can use the 'time position' of the temporal fringes as a measurement of the relative phase.

On average, the difference in the number of atoms detected at each port per time interval is given by

$$D(t)/\Delta t = \langle\psi_c(t)|C_1^\dagger C_1|\psi_c(t)\rangle - \langle\psi_c(t)|C_2^\dagger C_2|\psi_c(t)\rangle \tag{5}$$

$$= \mathrm{i}\kappa\left(\langle a^\dagger b\rangle \mathrm{e}^{\mathrm{i}\Omega t} - \langle b^\dagger a\rangle \mathrm{e}^{-\mathrm{i}\Omega t}\right). \tag{6}$$

We can write

$$\langle a^\dagger b\rangle = |\langle a^\dagger b\rangle|\, \mathrm{e}^{\mathrm{i}\phi_{ba}(t)} \tag{7}$$

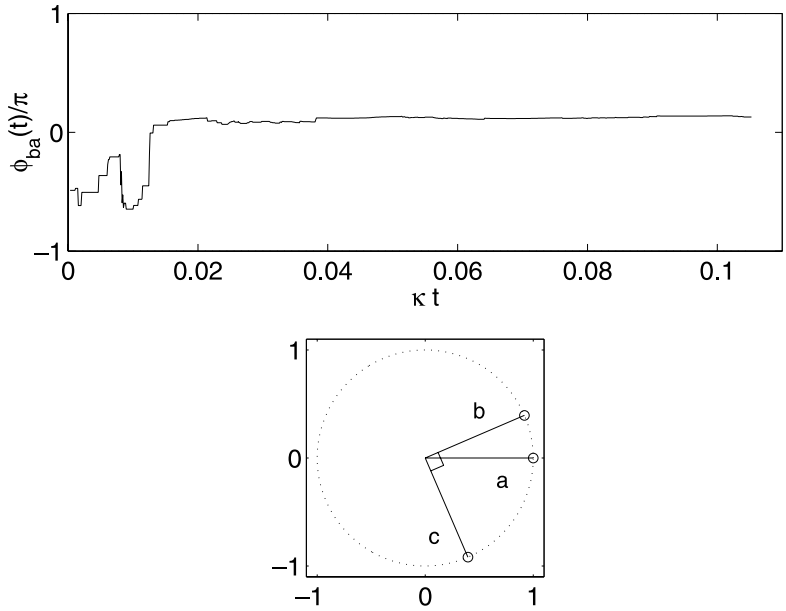

Figure 2. The time evolution of the relative phase between modes a and b is shown in (a) for $N = 1000$ and 10% of the atoms detected. The relative phase (modulo (2π)) is plotted against the dimensionless quantity κt, where κ is the rate of detection of atoms. A phasor diagram of the relative phases of the three modes after the Raman transfer for $\delta = 0$, is shown in (b). Mode a is used to set the zero of phase.

where $\phi_{ba}(t)$ contains the part that varies from realization to realization. With this substitution we obtain

$$D(t)/\Delta t = -2\kappa \sin(\Omega t + \phi_{ba}(t)). \tag{8}$$

So the relative phase is given by the argument of the sinusoidal plot of the difference in the number of atoms detected at each port per time interval. For our results, we subtract the known deterministic component, Ωt.

A plot of $\phi_{ba}(t)$ is shown in figure 2(a) for a system which initially has 1000 atoms in each trap and for which we detect about 10% of the atoms in the measurement process. As expected, the relative phase is initially undefined. Then, as atoms are detected, it fluctuates for a while before settling down to an approximately fixed constant value. This value is random and varies for measurements made on identically prepared systems.

2.3. Phase transfer

In the second part of this scheme, we coherently transfer a fraction of mode b, now entangled with the phase standard, a, to mode c, which is initially empty. Finally, we measure the relative phases between each of modes b and c with the phase standard, and thereby determine the relative phase between b and c.

The Hamiltonian for the transfer may be written as

$$H = \omega_b b^\dagger b + \omega_c c^\dagger c + \Gamma\left(bc^\dagger \mathrm{e}^{-\mathrm{i}\omega_{\mathrm{dr}}t} + b^\dagger c\, \mathrm{e}^{\mathrm{i}\omega_{\mathrm{dr}}t}\right) \tag{9}$$

where ω_{dr} is the driving frequency and the coupling strength, Γ, is real. For the sake of simplicity, in this section we are neglecting interactions between atoms. However,

these interactions, which lead to interesting effects such as collapses and revivals of the condensate phase [15], can readily be included in this formalism and we will reintroduce them in sections 4.2 and 4.3. In the interaction picture, we can write the Hamiltonian as

$$H_{\mathrm{I}} = \Gamma\left(c^{\dagger}b\exp\left(\mathrm{i}\delta t\right) + b^{\dagger}c\exp\left(-\mathrm{i}\delta t\right)\right) \tag{10}$$

where $\delta = \omega_c - \omega_b - \omega_{\mathrm{dr}}$ is the detuning between the driving and transition frequencies.

We define a new parameter, $\eta = t/t_0$, which is the coupling time (in practice, the duration of the transfer pulse), t, scaled by $t_0 = \pi/2\Gamma$, the time required to transfer the population completely from b to c. This parameter has the values $\eta = 0$ for no transfer, $\eta = 0.5$ for transfer of half of the population, and $\eta = 1$ for complete transfer. Rewriting equation (10) in terms of η, the time evolution operator, U_{bc}, to transfer from mode b to mode c is given by

$$\begin{aligned} U_{bc}(\eta, \delta, \Gamma) &= \exp\left(-\mathrm{i}H_{\mathrm{I}}t\right) \\ &= \exp\left(-\tfrac{1}{2}\mathrm{i}\eta\pi\left[c^{\dagger}b\exp(\mathrm{i}\pi\eta\delta/2\Gamma) + b^{\dagger}c\exp(-\mathrm{i}\pi\eta\delta/2\Gamma)\right]\right). \end{aligned} \tag{11}$$

The transfer is performed simply by operating on state (3) with (11). After this stage, we can write the state vector as

$$|\psi_c\rangle = \sum_{i,j} e_{i,j}|2N - l - i - j\rangle_a|j\rangle_b|i\rangle_c \tag{12}$$

where $\{e_{i,j}\}$ are coefficients determined by the numerical simulation.

Finally, we calculate the phases of the transferred and non-transferred components relative to the phase standard, respectively, ϕ_{ca} and ϕ_{ba}, and thereby determine the phase between b and c, ϕ_{bc}.

2.4. Results

To begin with, we consider the case where the transition between modes b and c is driven on resonance, $\delta = 0$. In this case, our simulations show that mode b always leads mode c by $\pi/2$, regardless of the strength of the coupling or the size of the fraction transferred. An example of this is shown in the phasor diagram of figure 2(b), where we have used a to fix the zero of phase, as is the role of the phase standard. As expected, the relative phase between a and b varies randomly from realization to realization, however, there is always a fixed phase difference of $\pi/2$ between b and c.

If we consider the case of two Josephson-coupled condensates without the phase standard, we obtain the same result. In this case, where mode b is initially in a number state, $|N\rangle$, and mode c is empty, $|0\rangle$, the phase is given by

$$\phi_{bc}(t) = \arg\left\{\langle 0|\langle N|\exp\left[\mathrm{i}\Gamma t\left(c^{\dagger}b + b^{\dagger}c\right)\right]c^{\dagger}b\exp\left[-\mathrm{i}\Gamma t\left(c^{\dagger}b + b^{\dagger}c\right)\right]|N\rangle|0\rangle\right\}. \tag{13}$$

This can be simplified, using the operator theorem [16]

$$\mathrm{e}^{\zeta B}A\mathrm{e}^{-\zeta B} = A + \zeta[B, A] + \frac{\zeta^2}{2!}[B, [B, A]] + \cdots. \tag{14}$$

After some algebra, equation (13) reduces to

$$\phi_{bc}(t) = \arg\left\{\tfrac{1}{2}\mathrm{i}N\sin(2\Gamma t)\right\}. \tag{15}$$

This shows that, for no interactions, all the atoms undergo independent Rabi oscillations. It is clear from (15) that $|\phi_{bc}|$ has the value $\pi/2$, for all times other than integer multiples of $t = \pi/(2\Gamma)$, at which times the phase is undefined. For $0 < t < \pi/(2\Gamma)$, c always lags b by

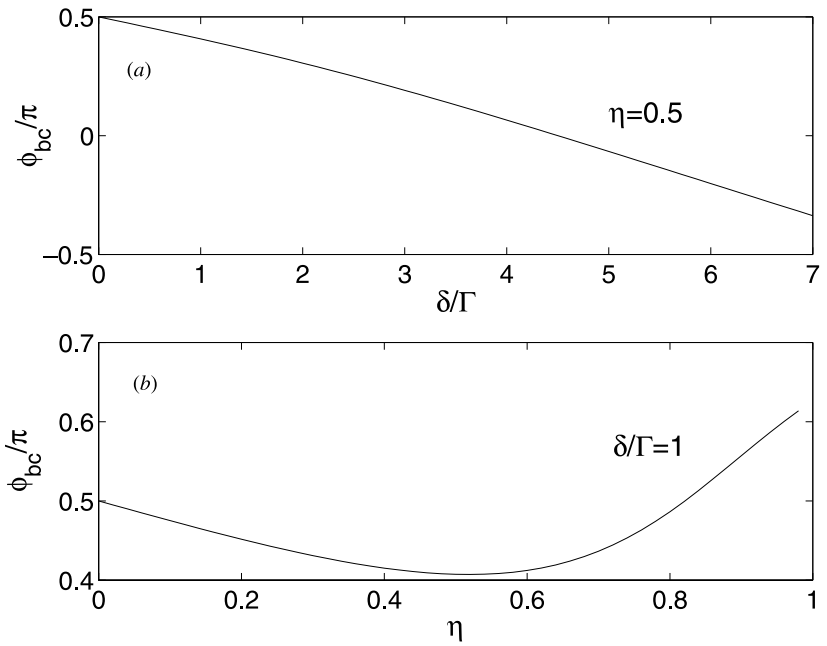

Figure 3. Plot of how the relative phase between b and c, ϕ_{bc} varies with (*a*) δ/Γ when $\eta = 0.5$, and (*b*) η when $\delta/\Gamma = 1$. All axes are unitless.

$\pi/2$, which is in agreement with our simulations. The times for which the phase is undefined are also easily explained as when all the population is in one mode. For odd multiples of $t = \pi/(2\Gamma)$, mode b is empty and mode c is in the number state $|N\rangle$, the converse is true for even multiples of $t = \pi/(2\Gamma)$. Clearly each of these situations has no phase information. The relative phase arises as soon as there is any entanglement between the modes, and is seen to always be $\pi/2$ for degenerate modes.

We can consider (11) to be the function of two variables: η and the ratio of the detuning to the coupling strength, δ/Γ. A plot of how ϕ_{bc} varies with η and δ/Γ is shown in figure 3. In figure 3(*a*), the transferred fraction is fixed at $\eta = 0.5$ and we plot how ϕ_{bc} varies with δ/Γ. In figure 3(*b*), we fix $\delta/\Gamma = 1$ and investigate how ϕ_{bc} varies with η. For no interactions between the atoms, these plots do not vary with atom number.

We find that the phase difference between modes b and c tends to $\pi/2$ (with mode b leading) independently in the limit of $\delta/\Gamma \to 0$ or $\eta \to 0$. The first limit corresponds to a detuning much smaller than the coupling strength. The second limit corresponds to a short coupling time, which is the case if only a very small fraction is transferred or if the coupling is very strong, $\Gamma \to \infty$.

For realistic systems, the interactions play an important role and we would need to include the effect of them in our calculation before making an accurate prediction of experimental results. However, keeping this in mind, we would like to get a feel for the expected phase difference by substituting parameters from a recent experiment.

Hall *et al* [11] have carried out a transfer of population and presented results for detunings of $\delta_1 = 2\pi \times 200$ Hz and $\delta_2 = 2\pi \times 350$ Hz. The coupling strength in their experiment was $\Gamma = 2\pi \times 625$ Hz and half of the population was transferred in each step, $\eta = 0.5$. Neglecting the effect of interactions, for $\eta = 0.5$ and $\delta_1/\Gamma = 0.32$, our simulation predicts a relative phase between b and c of $\phi_{bc}/\pi = 0.47$. For $\eta = 0.5$ and $\delta_2/\Gamma = 0.56$, we predict a relative

phase of $\phi_{bc}/\pi = 0.45$. Experimentally, the detuning can be varied readily, allowing control over the phase of the transferred component.

Figure 3 shows us that, with a careful choice of the parameters η and especially δ/Γ, we can transfer condensate components with the phase we want. This means that not only do we know that interference fringes will form in an interference experiment but that we can predict their positions.

3. Measurement-induced phase-locking

3.1. Introduction

We would now like to investigate how phase information is communicated along a chain of coupled condensates. This is of particular interest due to the recent experimental demonstration of a mode-locked atom laser [6]. In this experiment, condensates were trapped in the antinodes of an optical standing wave, and each site in this chain was coupled with its neighbours by quantum mechanical tunnelling. The output from the lattice was observed as a train of 'mode-locked' atomic pulses, demonstrating that each site has identical relative phases.

This study is relevant to the more general issue of how phase information is transported across a condensate of finite spatial extent. In particular, if the phase symmetry is broken at one point, does that induce symmetry breaking across the whole condensate?

We investigate condensates on spatially separated sites, coupled to their nearest neighbours. By breaking the symmetry at one of the end sites, we can see whether phase information is transported along the chain. In particular, we wish to see whether each mode acquires a fixed and predictable phase relationship with the end mode.

Recently, a study of a coupled two-mode system has been carried out using a semiclassical (mean-field) approach [17] and, among other things, predicts phase-locking of the condensate modes. Here, we perform a quantum calculation which also deals with the issue of how the phase symmetry is broken, rather than assuming *a priori* that each condensate can be assigned a phase.

3.2. Simulation of phase-locking

The system we consider consists of two condensates, b and c, which are Josephson-coupled. We make measurements which entangle one site with a phase reference condensate [4]. Our arrangement is very similar to that shown in figure 1. The only differences are that initially all the modes are in number states with the same number of atoms, and measurements of the interference pattern between a and b occur in the presence of Josephson coupling between b and c. In the previous section, we established a relative phase between a and b and, only after that was done, did we couple modes b and c.

Our simulation in section 2 can easily be modified for this system by including a Josephson coupling term in the system Hamiltonian. The coupling takes the same form as in the previous section, equation (10), with $\delta = 0$. With this inclusion, the system Hamiltonian becomes

$$H_0 = \omega_a a^\dagger a + \omega_b b^\dagger b + \omega_c c^\dagger c + \Gamma\left(b^\dagger c + c^\dagger b\right). \tag{16}$$

We need to perform a three-mode calculation rather than two two-mode calculations as in section 2. This slows down the calculation considerably and for this reason we consider only small atom numbers. For the simulations shown here, we consider 50 atoms in each trap. Halfway through each of the simulations, we turn the detections off and observe how the relative phase evolves under the influence of the Josephson coupling alone.

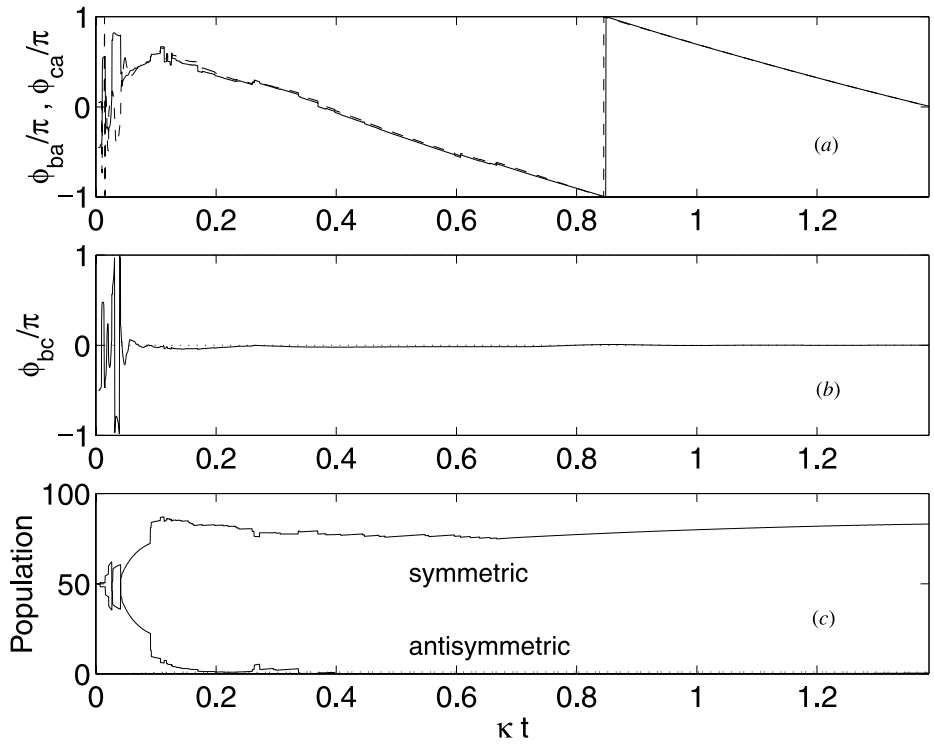

Figure 4. Demonstration of phase-locking. (*a*) Plot of the phases of modes b and c relative to the phase standard, ϕ_{ba} (full curve) and ϕ_{ca} (broken curve), as a function of time. (*b*) Plot of $\phi_{bc} = \phi_{ba} - \phi_{ca}$ against time. (*c*) Time variation of the populations in the symmetric and antisymmetric superpositions of the trap modes.

3.3. Results

Results are shown in figures 4 and 5. For our simulations, we consider modes b and c to be degenerate with $\omega_b/\Gamma = 5$. We take the frequency difference between a and b to be 40 times larger than the atomic detection rate, $\omega_b - \omega_a = 40\kappa$, and we detect about 30 atoms in each realization.

In figures 4(*a*) and 5(*a*) the relative phases between each of the condensates in the chain and the phase standard, ϕ_{ba} and ϕ_{ca}, are plotted as a function of time while the simulation takes place. In each case, we see that the relative phases jump around for a while before settling down. This is what we would expect while the relative phase between a and b is being established by the measurement process.

Eventually, the relative phases tend to a regular periodic pattern demonstrating a linear relationship between relative phase and time. This dependence is established while the detections are being made and continues after they are turned off. The discontinuities in figures 4(*a*) and 5(*a*) are simply due to the fact that we have plotted the relative phases modulo 2π.

The striking difference between these two results is that in figure 4(*a*) the phases of b and c lock to the same value relative to the phase standard, whereas in figure 5(*a*) they are completely out of step. This is illustrated more clearly in figures 4(*b*) and 5(*b*), where we have plotted the relative phase between modes b and c as a function of time, $\phi_{bc}(t) = \phi_{ba}(t) - \phi_{ca}(t)$. We see

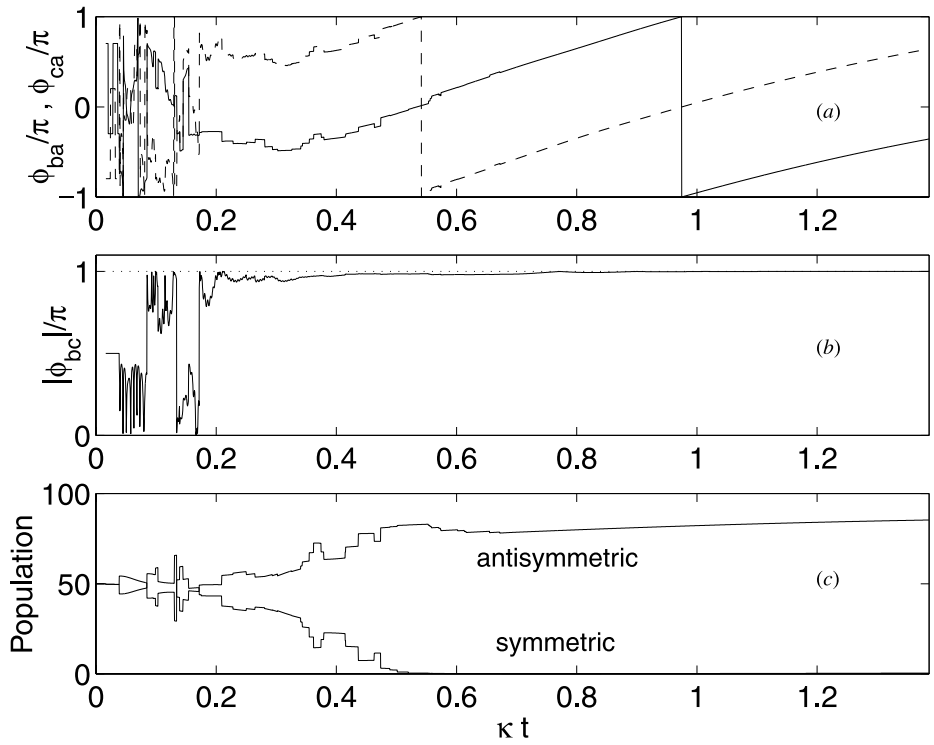

Figure 5. Demonstration of phase antilocking. (*a*) Plot of the phases of modes b and c relative to the phase standard, ϕ_{ba} (full curve) and ϕ_{ca} (broken curve), as a function of time. (*b*) Plot of $|\phi_{bc}| = |\phi_{ba} - \phi_{ca}|$ against time. (*c*) Time variation of the populations in the symmetric and antisymmetric superpositions of the trap modes.

that in figure 4(*b*), ϕ_{bc} oscillates for a while before settling to the constant value $\phi_{bc} = 0$, and in figure 5(*b*) $|\phi_{bc}|$ settles to π, that is the modes are exactly out of phase. All our simulations randomly give one of these two results: the phases of the two modes in the chain always either lock or antilock.

We can understand these results if we consider the eigenstates of the system. For a two-mode system with linear coupling and no interactions between atoms, the eigenstates are simply the symmetric and antisymmetric superpositions of the trap modes. If we write the trap wavefunctions for modes b and c, respectively, as ψ_b and ψ_c, then the eigenfunctions are $\psi_{\rm sym} = \psi_b + \psi_c$ and $\psi_{\rm asym} = \psi_b - \psi_c$. We can write this as

$$\psi = \psi_b + \mathrm{e}^{\mathrm{i}\phi}\psi_c \tag{17}$$

where $\phi = 0$ for the symmetric mode, $\psi_{\rm sym}$, and $\phi = \pi$ for the antisymmetric mode, $\psi_{\rm asym}$. The eigenstates correspond to the phases of the two traps either being in phase or antiphase. An analogy can be drawn with two coupled pendulums. The normal modes for this system are those where the pendulums swing perfectly in step or half a cycle out of phase.

The tendency for the system to occupy one of the eigenstates is shown in figures 4(*c*) and 5(*c*). In these, we have plotted the populations of the symmetric and antisymmetric eigenstates as a function of time. In figure 4(*c*), we see that the population of the antisymmetric mode vanishes and all the atoms occupy the symmetric mode. This is consistent with the fact that

the relative phase between modes b and c tends to zero. The converse is true in figure 5(c): all the atoms occupy the antisymmetric mode and the relative phase between b and c tends to π. We will discuss these results using a semiclassical model in the next section.

It is not surprising that a phase relationship develops between the modes. The coupling between b and c, when we measure the interference pattern between a and b, means that we do not know from which of the three modes a detected atom has come. This leads to entanglement between all three condensates.

3.4. Comparison with a semiclassical model

A useful way to understand these results is to perform a semiclassical analysis of the system. Such an approach is only approximate and requires that we make certain assumptions, such as each condensate initially having a well defined phase. Nonetheless, it is a powerful technique for understanding the dynamics of the system and has allowed previous authors to predict interesting features such as π-oscillations and macroscopic quantum self-trapping [18]. Following a similar approach, for degenerate modes and non-interacting atoms, the equations of motion for the system are

$$\dot{z}(t) = -2\Gamma\sqrt{1 - z^2(t)}\sin(\phi(t)) \tag{18}$$

$$\dot{\phi}(t) = 2\Gamma\left(\frac{z(t)}{\sqrt{1 - z^2(t)}}\right)\cos(\phi(t)) \tag{19}$$

where $\phi(t)$ is the phase of mode b relative to c, and we have defined the quantity of fractional population imbalance, $z(t) \equiv (N_b(t) - N_c(t))/N$, where N_b and N_c are the numbers of atoms in modes b and c, and N is the constant total number of atoms.

The stationary solutions of this system are $\phi = 2n\pi$, $z = 0$ and $\phi = 2(n + 1)\pi$, $z = 0$, where n is an integer. We see that the two stationary solutions are when the populations in each trap are equal and the phases (modulo (2π)) are either in step or half a cycle out of step. That is, the stationary solutions are the symmetric and antisymmetric eigenstates of the system. This is in agreement with the results of our simulations.

We can perhaps see this more clearly by linearizing (19) in z,

$$\ddot{\phi} = -\tfrac{1}{2}\sin(2\phi(t)) - z(t)\sin(\phi(t)) + \mathcal{O}(z^2). \tag{20}$$

This is justified since, for non-interacting atoms, our simulations show that if the traps initially have equal populations, the populations remain very nearly equal for all time, i.e. $|z(t)| \ll 1$. Following the argument of Raghavan *et al* [18], this suggests a mechanical analogy in which a particle, of mass unity, with spatial coordinate ϕ moves in the potential

$$V(\phi) = -\tfrac{1}{4}\cos(2\phi) - z\cos(\phi) + \mathcal{O}(z^2) \tag{21}$$

which has local minima at $\phi = 0$ as well as $\phi = \pm\pi$, and confirms the results of our simulations.

Our simulations show that for non-zero interactions between atoms, the relative phase between the traps depends on the sign of the interaction. For repulsive interactions, the system tends towards the symmetric mode with zero phase difference between the traps (a typical trajectory looks like figure 4). Conversely, for attractive interactions, the system tends to the antisymmetric mode with π phase difference (a typical trajectory looks like figure 5). This agrees with the semiclassical approach of Raghavan *et al* [18].

4. Natural phase-locking

4.1. Dissipation

In the previous section, we observed phase-locking along a chain of condensates when a phase was established between the end sites by measurement. In the experiment of Anderson and Kasevich [6], however, no such measurement was made. We would like to understand the mechanism by which the phases could lock in this case. We begin, in this section, by considering the effect of dissipation at one of the sites. In the following sections, we will consider interactions and then the combined effect of interactions and loss.

We begin by calculating the relative phase for a two-mode system with no loss and with each mode initially in the same number state. The phase between modes a and b is given by

$$\phi_{ba}(t) = \arg\left\{\langle N|\langle N|\, U_{ab}^{\dagger}(t)\, a^{\dagger}b\, U_{ab}(t)\, |N\rangle|N\rangle\right\} \tag{22}$$

where

$$U_{ab}(t) = \exp\left[-\mathrm{i}\Gamma t\left(a^{\dagger}b + b^{\dagger}a\right)\right] \tag{23}$$

if the modes are degenerate. This can be simplified, using (14), to give

$$\begin{aligned}\phi_{ba}(t) &= \arg\left\{\tfrac{1}{2}\langle N|\langle N|\left[\mathrm{i}\left(b^{\dagger}b - a^{\dagger}a\right)\sin(2\Gamma t) + \left(a^{\dagger}b - b^{\dagger}a\right)\cos(2\Gamma t) + b^{\dagger}a\right]|N\rangle|N\rangle\right\} \\ &= \arg\{0\}\end{aligned} \tag{24}$$

which is undefined for all time, i.e. the system has no phase information. In fact, a more general definition of phase [14] shows that phase information does exist for this system, but cycles with time. At odd multiples of $\pi/4\Gamma$, the relative phase between the modes is zero, and at even multiples of $\pi/4\Gamma$, the relative phase is undefined. We are only interested in the case where the phase stabilizes with time. However, when dissipation is introduced at one site (or both sites), the number symmetry of the system is broken and, as we shall see below, a stable relative phase can develop between the modes.

For our simulations, we consider a chain of three condensates, all initially in number states with the same number of atoms. Each mode is coupled to its neighbours by quantum mechanical tunnelling (see figure 6).

We use a quantum jump method (as outlined above) to simulate the loss process from mode a. A phase will not be established if the modes are degenerate. For simplicity, we take the mode frequencies to be in the ratio $\omega_a : \omega_b : \omega_c = 1 : 2 : 3$. We take the ratio of the mode couplings to the trap frequencies as $\Gamma/\omega_a = 0.1$ and the ratio of the detection rate to the trap

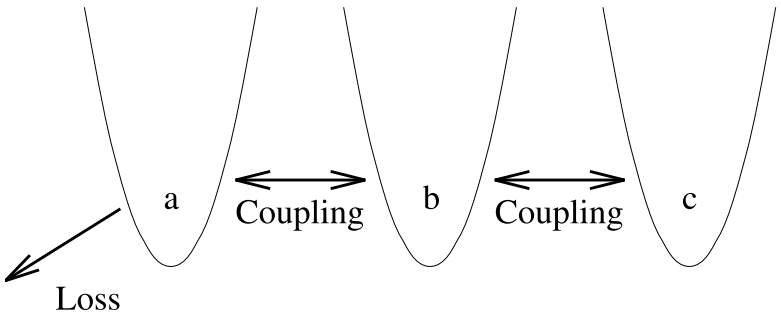

Figure 6. Chain of coupled condensates. Each pair of adjacent condensates is coupled by quantum mechanical tunnelling and there is dissipation from mode a.

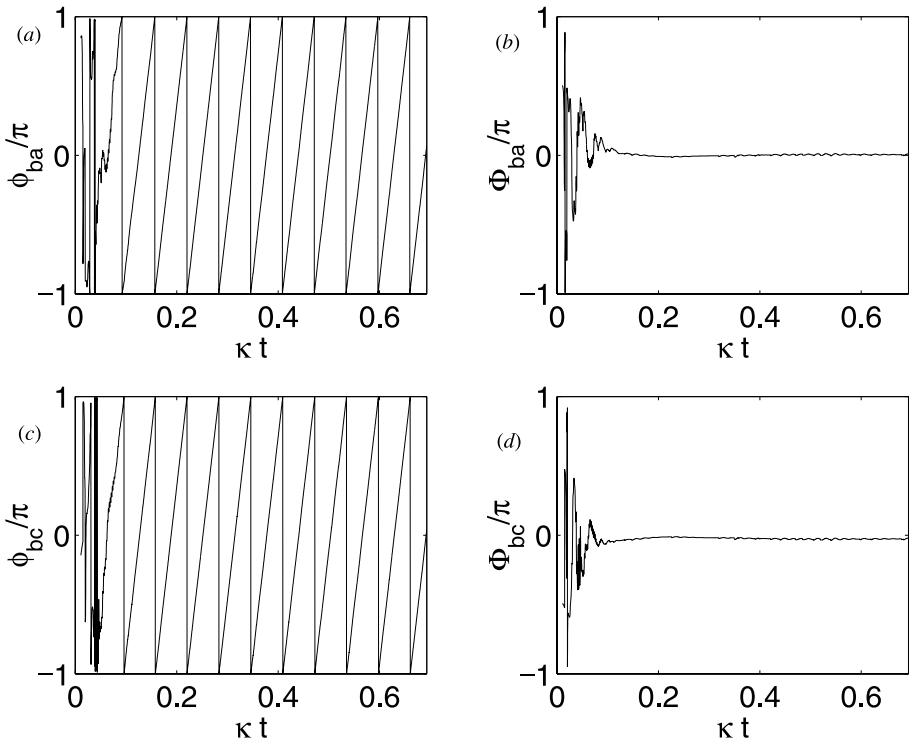

Figure 7. Phase-locking due to dissipation. In each figure we have plotted phase against the dimensionless quantity κt: (*a*) ϕ_{ba}; (*b*) ϕ_{ba} with the deterministic part removed; (*c*) ϕ_{bc}; (*d*) ϕ_{bc} with the deterministic part removed. There are initially 50 atoms in each mode.

frequencies as $\kappa/\omega_a = 0.01$. This means that the loss rate is much smaller than the coupling frequency which is, in turn, much smaller than the trap frequencies. We take $N = 50$, i.e. each trap is initially in a number state with 50 atoms. Typically about 30 atoms are lost from mode a for each trajectory. To begin with, we ignore interactions between atoms.

The result of a simulation for a single trajectory is shown in figure 7. In figure 7(*a*) we have plotted the relative phase between modes a and b. As expected, the phase is initially undefined, which corresponds to the time before an atom is lost from the trap. However, once an atom has been lost, a phase develops between the modes. We see in figure 7(*a*) that this is initially unstable and fluctuates for a while before settling down to a steady linear relationship with time. The discontinuities in this plot are purely an artefact of plotting the phase modulo 2π.

The linear relationship in the plot is due to the fact that there is a frequency difference between modes a and b. We would expect there to be a deterministic component of the relative phase dependent on $\omega_b - \omega_a$, which allows us to write the time dependence of the relative phase as

$$\phi_{ba} = (\omega_b - \omega_a)\, t + \Phi_{ba} \tag{25}$$

where Φ_{ba} accounts for the stochastic non-deterministic part and can be thought of as the ϕ_{ba}-axis intercept if we were to fit a line to the linear part of the plot. In figure 7(*b*), we have plotted the time dependence of Φ_{ab}. This fluctuates for a while before settling to zero. The

corresponding results for modes b and c are shown in figures 7(c) and (d) and we see that we obtain very similar results.

In this case, we do not detect atoms as they are lost from the condensate and so do not know the times at which they escape. This means that, unlike previous cases which deal with direct detection [4], we need to average over all trajectories. This is equivalent to using a density matrix description which formalizes our uncertainty of the escape times.

The relative phase between the condensate modes is given, in terms of the density matrix, as

$$\phi_{ba}(t) = \arg\left[\mathrm{Tr}\left\{\rho(t)a^{\dagger}b\right\}\right]. \tag{26}$$

It is straightforward to show that the time dependence of the phase of our system is given by simply averaging over the relative phases of individual trajectories.

We might expect that each trajectory will settle to a well defined phase, but that this phase will vary randomly from run to run. This would mean that on the ensemble average the phase information would be wiped out, which was the interpretation of the results in the papers for which a relative phase was established by measuring the interference pattern between two condensates [1]. In our case, however, a remarkable thing happens. In figures 7(a) and (c), the results of each trajectory are random and different for the initial fluctuating time, but then they always overlap in the linear region. This is seen more clearly in figures 7(b) and (d) when the deterministic part of the phase has been removed. We see that, although random to begin with, every trajectory rapidly settles to zero phase difference between the modes.

This means that each trajectory is the same as the ensemble average, at least in the long-time limit. In other words, we have a system for which the phase persists even in the ensemble average. This is a remarkable result: our uncertainty in the times of the loss of the atoms does not wipe out the phase.

The establishment of phase can be explained in a similar way to that of Javanainen and Yoo [1]. Although all the atoms are removed from a, the modes are all coupled, so we do not know which mode the atom has come from. This uncertainty leads to entanglement and the establishment of a relative phase.

4.2. Interactions

Up until now, we have ignored an effect that will be present in any realistic system: nonlinearities in the Hamiltonian due to the interactions between atoms. In this section, we neglect dissipation and consider the effects of interactions alone.

This is easily simulated within the existing framework by setting the rate of loss to zero and introducing nonlinear terms to the system Hamiltonian. The full three-mode Hamiltonian including interactions and coupling becomes

$$H_0 = \omega_a a^{\dagger}a + \omega_b b^{\dagger}b + \omega_c c^{\dagger}c + \Gamma\left(a^{\dagger}b + b^{\dagger}a + b^{\dagger}c + c^{\dagger}b\right) + U\left(a^{\dagger 2}a^2 + b^{\dagger 2}b^2 + c^{\dagger 2}c^2\right) \tag{27}$$

where U is the interaction strength. For simplicity, we have assumed that the coupling strength is the same between both pairs of modes and that the same is true of the interaction within each mode. We will take the modes to be degenerate $\omega_a = \omega_b = \omega_c \equiv \omega$. The evolution for this system is deterministic and so we can evolve a state in time by direct integration.

We use the experimental parameters of the experiment of Anderson and Kasevich [6]. In this case, the kinetic energy per particle is $E = k_{\mathrm{B}} \times 157$ nK, the interaction energy per particle is $\tilde{U} = k_{\mathrm{B}} \times 4$ nK, and the wavelength of the optical standing wave that forms the lattice is

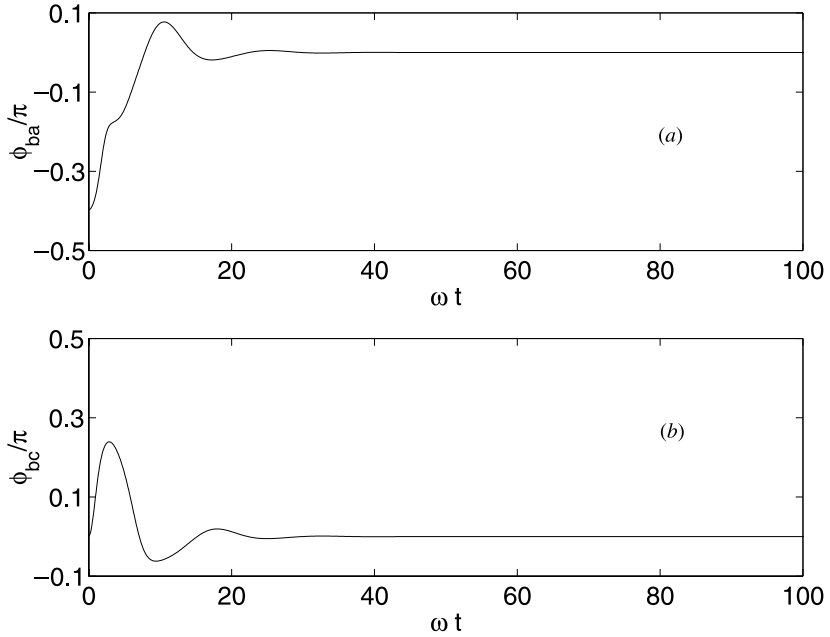

Figure 8. Phase-locking due to atomic interactions. In each case, the phase is plotted against ωt (i.e. the number of trap oscillations).

$\lambda = 850$ nm. From these, we can determine the ratio of the interaction energy per particle to the kinetic energy per particle, $\tilde{U}/E \approx 0.03$, and, by assuming that the well depth, ϵ, is approximately equal to the kinetic energy per particle, E, we can find the coupling rate per oscillation

$$\frac{\Gamma}{\omega} \approx \exp\left(\frac{-\lambda E}{8\hbar^2 g}\right) \approx 0.01. \tag{28}$$

This means that for our simulations, we take $U/N\omega = 0.03$ and $\Gamma/\omega = 0.01$. As was shown in equation (24), we need to start with a different number of atoms in each of the modes.

The result of a simulation, for modes a, b and c initially having 50, 49 and 48 atoms, respectively, is shown in figure 8. We see that the relative phase between each pair of modes rapidly damps to zero. For the parameters we use here, it takes about 30 trap oscillations to stabilize to zero relative phase. Other simulations demonstrate that the rate of damping increases with the interaction energy. For repulsive interactions, the modes lock in phase and for attractive interactions, the modes antilock. This is consistent with the results for measurement-induced phase establishment.

Our results show that interactions (as well as dissipation) when combined with Josephson coupling between condensates, establish a phase. This can be explained by the modes becoming entangled due to the coupling. Interactions have the advantage of establishing a phase for degenerate modes. Unlike the case of dissipation, however, there must be a number asymmetry between the modes in the initial state. Ideally, we would like a scheme that supports both, so that a phase 'naturally arises' for the most symmetric initial case.

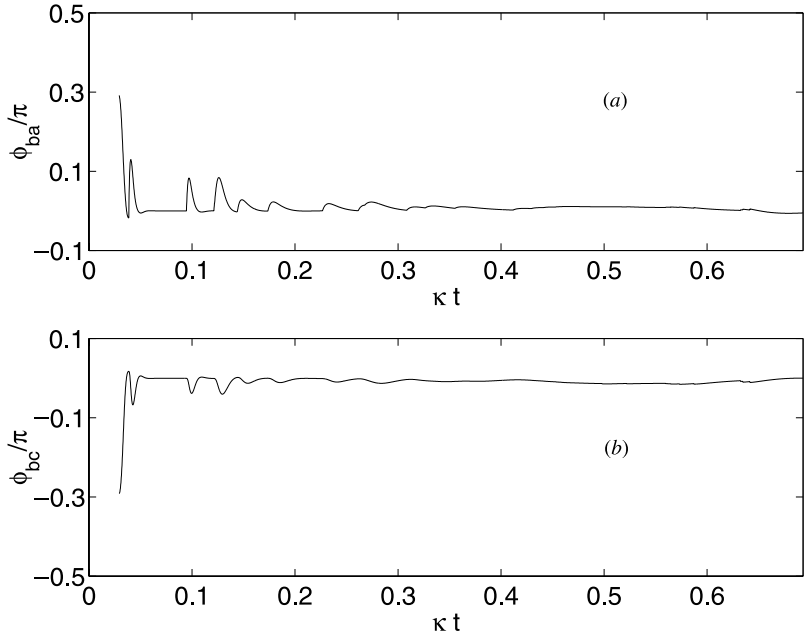

Figure 9. Phase-locking due to interactions and dissipation. There are initially 50 atoms in each mode and the system parameters closely match experiments (see text). The phase is plotted against the unitless quantity κt.

4.3. Dissipation and interactions

In a full realistic model, there will be interactions between atoms as well as dissipation from the condensate modes. In this section, we wish to see whether, by including both effects, phase-locking arises for all cases: notably for the most rigorously symmetric case of degenerate modes in equal number states.

Our simulation process is the same as in section 4.1, but with the nonlinear terms included in the Hamiltonian, as in (27). We take the experimental parameters as outlined in section 4.2, with the dissipation rate as an additional parameter. It was noted in [6] that this rate was much smaller than the coupling rate. So, for our simulations, we take $\kappa/\omega = 0.001$.

When we include dissipation as well as interactions, we can start with degenerate modes each in the same number state. The result for one trajectory, with 50 atoms initially in each mode, is shown in figure 9. For repulsive interactions, the modes lock in phase for each trajectory. This means that the phases lock on the ensemble average and we do not have to make a measurement for this process to occur. For attractive interactions, the phases of adjacent modes antilock. Again, this is consistent with our previous results.

We see that the phase-locking is not as rapid or as clean as for the case of interactions alone. For the parameters used here, it takes about 300 trap oscillations for the phases to lock as compared with about 30 for no dissipation. This can be explained by the fact that the dissipation corrupts the entanglements between the modes and so degrades the phase relationship between them.

Since we have shown that phases lock (or antilock) for the most symmetric system, we know that this is true for all initial states. We have shown that Josephson-coupled condensate modes with repulsive interactions and dissipation will always lock in phase, *independent of*

the initial state. This is a powerful result and explains the experimental observations of the mode-locked atom laser [6].

5. Conclusions

We have seen that a transfer of population between two modes leads to a relative phase between them due to entanglement and that this phase is not necessarily zero. A study of this transfer process shows how we could predict and control the phase of the output pulses from an atom laser and the position of interference fringes in interferometry schemes involving condensates.

By extending these ideas, we have studied the effect on a chain of coupled condensates of making measurements which establish a phase at one of the lattice sites. Our simulations show that the system always relaxes into one of the eigenstates of the system and which eigenstate this is depends on the sign of the interatomic interactions. These results should be able to be extended to a long chain of condensates, which may allow us to demonstrate a mechanism by which phase information is transported across a condensate with finite spatial extent.

Finally, we have considered mechanisms by which a phase naturally arises for the case of degenerate modes initially in equal number states. We have found that dissipation alone is enough to lock the phases for all but the case of degenerate modes and that atomic interactions alone are enough for all but the case of equal atom numbers. By combining these, we have seen that phase-locking occurs for all systems where both processes are present.

Our findings in this last section are threefold. Firstly, by considering a model that closely matches the mode-locked atom laser of Anderson and Kasevich, we have demonstrated a mechanism by which the phases of the condensate modes lock and that this is completely independent of the initial state of the system. Secondly, we have demonstrated a system where the phase persists even on the ensemble average. Thirdly, we have provided an example of a system for which we would expect relative phases to occur naturally due to dissipation and interactions. This is in agreement with observation of such systems and is a significant advance on previous proposals which have required a measurement on a pair of condensates to *create* a relative phase between them.

Acknowledgments

This work was financially supported by the British Council, the United Kingdom EPSRC and the EU, under the TMR network 'Coherent Matter Wave Interactions' ERB-FMRX-CT-0002.

References

[1] Javanainen J and Yoo S M 1996 *Phys. Rev. Lett.* **76** 161
[2] Castin Y and Dalibard J 1997 *Phys. Rev.* A **55** 4330
[3] Jack M W, Collett M J and Walls D F 1996 *Phys. Rev.* A **54** R4625
[4] Dunningham J A and Burnett K 1999 *Phys. Rev. Lett.* **82** 3729
[5] Stamper-Kurn D M *et al* 1998 *Phys. Rev. Lett.* **80** 2027
[6] Anderson B P and Kasevich M A 1998 *Science* **282** 1686
[7] Josephson B D 1962 *Phys. Lett.* **1** 251
[8] Matthews M R *et al* 1998 *Phys. Rev. Lett.* **81** 243
[9] Featonby P D *et al* 1998 *Phys. Rev. Lett.* **81** 495
[10] Mewes M-O *et al* 1997 *Phys. Rev. Lett.* **78** 582
[11] Hall D S, Matthews M R, Wieman C E and Cornell E A 1998 *Phys. Rev. Lett.* **81** 1543
Hall D S, Matthews M R, Wieman C E and Cornell E A 1998 *Phys. Rev. Lett.* **81** 1539

[12] Hagley E W *et al* 1999 *Science* **283** 1706
[13] Carmichael H J 1993 *An Open Systems Approach to Quantum Optics* (Berlin: Springer)
Dalibard J, Castin Y and Mølmer K 1992 *Phys. Rev. Lett.* **68** 580
Gisin N and Percival I 1992 *Phys. Lett.* A **167** 315
Gisin N and Percival I 1992 *J. Phys. A: Math. Gen.* **25** 5677
[14] Pegg D T and Barnett S M 1989 *Phys. Rev.* A **39** 1665
[15] Wright E M, Walls D F and Garrison J C 1996 *Phys. Rev. Lett.* **77** 2158
[16] Louisell W H 1973 *Statistical Properties of Radiation* (New York: Wiley)
[17] Smerzi A, Fantoni S, Giovannazzi S and Shenoy S R 1997 *Phys. Rev. Lett.* **79** 4950
[18] Raghavan S, Smerzi A, Fantoni S and Shenoy S R 1999 *Phys. Rev.* A **59** 620